Bull. Mater. Sci. (2020) 43:98
https://doi.org/10.1007/s12034-020-2067-y

Improved thermal stability and oxidation resistance of electrodeposited NiCrP amorphous alloy coatings

Y Q GUO, J K YU*, H B YANG, Q QIAO, Q Y LI and X C ZHAO
State Key Laboratory of Metastable Materials Science and Technology, Yanshan University, Qinhuangdao 066004, Hebei, People's Republic of China
*Author for correspondence (yujinku@ysu.edu.cn)

MS received 30 July 2019; accepted 20 January 2020

Abstract. Amorphous NiP and NiCrP alloy coatings were prepared on copper substrates by electrodeposition. The thermal stability of the obtained coatings were evaluated by the onset temperature of phase transformation identified with differential scanning calorimetry measurements, and their high temperature oxidation resistances were characterized by the oxidation kinetics curve and the oxidation activation energy. The mechanism of the doping effect of Cr element on crystallization temperature and oxidation resistance of the alloy coatings were discussed based on X-ray diffraction analysis. The results show that the crystallization temperature of NiP amorphous alloy was 344°C, and the oxidation activation energy was calculated to be 1.54×10^3 J mol^{-1}. As for NiCrP alloy coating with a Cr content of 1.8 wt%, the crystallization temperature increased to 403.8°C and the calculated oxidation activation energy was 3.53×10^4 J mol^{-1}, 2.29 times higher than the NiP coating. The remarkably enhanced high-temperature oxidation resistance of NiCrP alloy coating can be attributed to the compact metal oxide film formed on the surface.

Keywords. NiCrP alloy coating; thermal stability; high-temperature oxidation resistance; microstructure; crystallization behaviour.

1. Introduction

NiP amorphous alloy has been widely used in the aerospace industry, i.e., the coatings on engine impellers and substrate of compressor, due to its impressive wear resistance, corrosion resistance and low cost [1–9]. Some of the core components of the engine usually work under a moderate servicing condition of 300−500°C but bearing continuous heating-cooling cycles, which will lead to the inevitable degradation of their gas-corrosion performance. Therefore, besides the required corrosion and wear resistances, the fabricated amorphous alloy coating must possess the excellent thermal stability and high-temperature oxidation resistance. However, NiP amorphous alloys are thermodynamically metastable, and will gradually transform to the stable crystalline phase, leading to the severe deterioration or even elimination of their key performance. Therefore, it is highly imperative to improve the thermal stability and oxidation resistance of NiP amorphous alloy coatings.

It is known that the performance of amorphous NiP coating can be improved by adding one or more alloy elements. For example, the addition of Co [10] and Fe [11] elements to the alloy coating can change its catalytic performance, meeting the rigorous servicing requirements. The added Co element can improve the wear resistance and hardness of the amorphous alloy coating, and the addition of W element [12] can greatly improve the friction and wear performance. Nevertheless, in order to improve both the thermal stability and high temperature oxidation resistance, it is necessary to consider other specific element with a high melting point. Furthermore, the appropriate element should have a large atomic radius, by which the diffusion of the added atoms can be effectively hindered, and thus increasing the barrier potential of the unwanted amorphous-crystalline phase transition. From this point of view, Cr could be an ideal element due to its high melting point and relatively large atomic volume; it can further form a dense oxidation film at high temperature to protect the internal oxidation of the alloy coating [13,14]. Therefore, in this study Cr element has been selected as the addition element to improve the thermal stability and oxidation resistance of the amorphous alloy coating.

There are many methods [15–17] for the preparation of NiCrP amorphous alloy coatings, among which electroplating and electroless plating are more economical and have broad industrial application prospects. Compared with the electroless plating method, the electroplating process is easy to control with a longer bath time, the composition of the electrolyte is simple and low-cost, and the deposited coating is of a high stability. Hitherto, few studies have been focused on the high-temperature oxidation resistance of the electroplated amorphous NiCrP alloy coating. The thermal stability and oxidation resistance is of great significance to

Published online: 25 March 2020

understand the failure mechanism of the coatings under high temperature.

2. Experimental

Both of the binary NiP and ternary NiCrP coatings were deposited on pure copper substrates by electrodeposition. At first, the substrate was machined to the dimension of $12 \times 12 \times 2$ mm^3, and then immersed in a mixed aqueous solution of 15 g l^{-1} NaOH, 25 g l^{-1} Na_2CO_3, 25 g l^{-1} Na_3PO_4, and 1 ml l^{-1} of OP-10 to remove the cutting oils, followed by a through wash in the hot water (60−70°C) and cold water, respectively. Subsequently, the cleaned substrate was immersed in a mixed acid solution of 50 g l^{-1} phosphate, 20 g l^{-1} nitric acid and 30 g l^{-1} acetic acid for polishing, further etched in a 160 ml l^{-1} H_2SO_4 and 80 ml l^{-1} H_2O_2 solution for 10 min, and finally washed with deionized water. The following electrolyte was used for electrodeposition: 5 g l^{-1} $NiSO_4 \cdot 6H_2O$, 100 g l^{-1} $CrCl_3 \cdot 6H_2O$, 1 g l^{-1} $NaH_2PO_2 \cdot H_2O$. Analytical reagents and deionized water were used to prepare the plating bath, the pH value of the electrolyte was adjusted to 3.5 by using 5 g l^{-1} NaOH or 10 g l^{-1} H_2SO_4. During the plating process, a piece of copper was used as the cathode, the current density (D_K) was 15 A dm^{-2}, and the temperature was maintained at 30°C. The substrate was placed in a cell equipped with a numerical control double-polar pulsed electrical source (SMD300/50, Handan Dashun, China). Coating composition was controlled by adjusting bath composition and process parameters. The approximate range of bath composition and process parameters was first selected by orthogonal test. Then the influences of single factor on the coating surface quality, coating composition, coating structure and coating performance were analysed in detail, and the optimal bath composition and process parameters are finally determined and the best alloy coating was obtained. After the electrodeposition, the obtained coating was peeled off from the substrate and stored in a desiccator for further use. The weight of the peeled NiP and NiCrP coatings was in the range of 500–1000 mg, and their thickness was generally 100−200 μm.

A HS-4800 field emission electron microscope (Hitachi, East Coast Port City, Honshu Island) attached with a INC 250 spectrometer (EDS) was used to analyse the content of alloy coatings.

Thermal analyses (sample weight 8–10 mg, heating rate of 10 K min^{-1}) and isothermal oxidation tests of the amorphous alloy coatings were carried out in a STA449C/6/G differential scanning calorimeter (DSC; Erich NETZSCH GmbH & Co. Holding KG, Germany) with α-Al_2O_3 crucibles at 300, 400 and 500°C, respectively. Before the DSC measurements of the alloy coatings, the temperature and energy were calibrated by standard materials, such as Al at the identical heating rate (10 K min^{-1}). As for the thermal stability and oxidation resistance measurements of the alloy samples, the heating process was conducted under a high-purity argon gas protection with a flowing rate of 35 ml min^{-1}; when the temperature was near the target value (usually 20°C lower than the heat preservation temperature), the heating rate is decreased to 2 K min^{-1} and the atmosphere was changed to be air, and then a heat preservation was for 10 h.

The phase composition of the obtained alloy coatings before and after oxidation was characterized by an X-ray diffractometer (XRD; D/MAX2500HB+/PC, Rigaku, Akishima, Tokyo, Japan) using Cu Kα radiation (λ = 0.154178 nm) with a scanning rate of 2° min^{-1} and a scanning step of 0.02° . The alloy coatings were cut into 10 × 10 mm^2 square pieces by using a wire-cutting machine for XRD measurements.

3. Results and discussion

The compositions of coatings were determined to be Ni (89.13 wt%) and P (10.87 wt%) for NiP; Ni (88.66 wt%), P (10.54 wt%), Cr (0.80 wt%) for NiCr0.80P; Ni (87.96 wt%), P (10.24 wt%) and Cr (1.80 wt%) for NiCr1.80P, respectively. The thickness for the coatings was controled to be about 120 μm.

Figure 1 shows the DSC curves of NiP and NiCrP amorphous alloy coatings. It can be seen that the exothermic onset temperature of the NiP alloy coating appears at 344.1°C, while that of the NiCrP alloy coating is at 375.4−403.8°C. The measured results are consistent with that reported in the previous works [3,18]. As the temperature increases, the phosphorus atoms in the amorphous coating start to migrate and diffuse, leading to the phase transition to a thermodynamically stable crystalline state. Even for a trace content of Cr (0.5 wt%) being added into the alloy coating, the crystallization onset temperature showed a notable increase. When the Cr content reached 1.80 wt%, the crystallization starting temperature further increased to 403.8°C. Wang and Lu [19] reported that the short-range ordered structure (i.e., ordered atomic group)

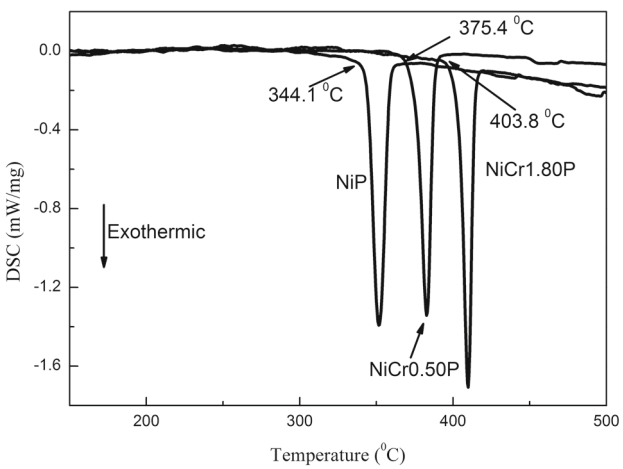

Figure 1. DSC curves of NiP and NiCrP amorphous alloy coatings.

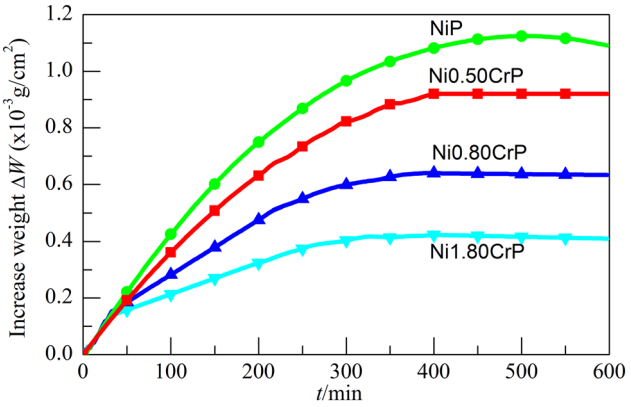

Figure 2. Isothermal oxidation curves of NiP and NiCrP alloy coatings at 400°C.

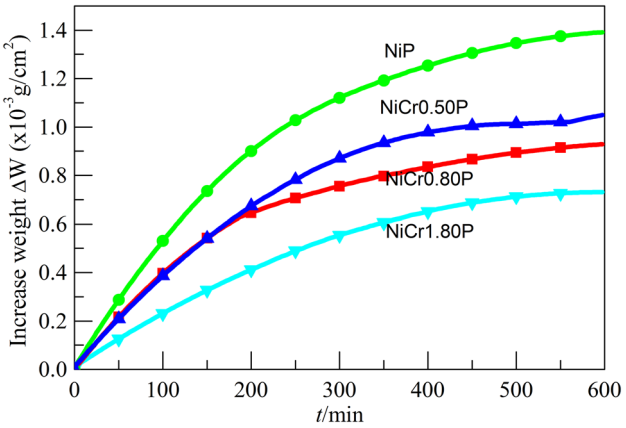

Figure 3. Isothermal oxidation curves of NiP and NiCrP alloy coatings at 500°C.

in amorphous alloys has a significant influence on the crystallization process. Generally, a more ordered atomic group results in a lower crystallization temperature, and smaller activation energy and Aurami index of the crystallization process. According to this theory, since the Cr element has a high melting point, the positional energy needed for amorphous–crystalline phase transition will be increased by adding Cr in the alloy coating, effectively hindering the atomic diffusion process. As a result the short-range ordered structure becomes less, leading to an increased crystallization temperature of the NiCrP alloy coating.

The oxidation resistances of the deposited alloy coatings at different temperatures are directly dependent on their composition and the specific oxidation temperatures. Therefore, we have measured the oxidation kinetics curves of the amorphous NiCrP alloy coatings with different Cr contents at different temperatures to investigate the effects of Cr and oxidation temperature on the oxidation resistance behaviours of the amorphous alloy coatings.

In general, the high-temperature oxidation of the alloy coating can be divided into three stages: namely, the surface rapid oxidation stage, the oxide film formation stage, and the steady state with the formation of a dense oxide film. Figures 2 and 3 show the relationship between the oxidation weight gain and the preservation time of the alloy coating measured at 400 and 500°C, respectively. It can be observed that the change trend of the oxidative weight gain curve is very similar. At the initial stage of oxidation the oxidative weight gain shows a fast increase known as the rapid oxidation stage, because the unoxidized alloy and the oxidizing medium are relatively sufficient. After this stage, an oxide film will be formed on the surface of the alloy coatings, while the compactnesses of the oxide films could exhibit a vibration for different alloy coatings. The formed oxide film can isolate the oxygen from the matrix of the alloy coating, slowing down the oxidation rate. When the formed oxide film is dense enough, the weight gain of the alloy coating tends to be a stable value, and the actual mass growth tends to be very gentle, indicating the appearance of the steady state. If the oxide film formed on the coating surface is not dense (caused by the defects such as pores, cracks, etc.), the weight gain of the alloy coating will continuously increase.

Figure 2 shows the oxidation weight gain curves of the alloy coatings with different Cr contents at 400°C. It can be seen that the oxidation kinetics curves of the four alloy coatings show an approximate exponential increase, clearly representing the three stages of the oxidation process as mentioned above.

When the mass fraction of Cr in the alloy coating exceeds 0.8 wt%, it enters the steady-state phase more quickly. This suggests that a dense oxide film can be formed to prevent the coating matrix from further oxidation, and the alloy coating can be well protected.

The weight gain curve of the NiP alloy coating is higher than those of the other three alloy coatings. However, the curves of the NiP and Ni0.5CrP alloy coatings are quite close, which means at the oxidation temperature of 400°C, the formed Ni oxide film on the coating surface may play a major role for hindering further oxidation, as the Cr content in the coating is small. When the Cr content in the alloy coating becomes larger, the final oxidation weight gain becomes smaller, in which the Cr oxide plays the major isolation role.

The main reason for this phenomenon is that Ni is located after Cr in the periodic table of elements, and has similar physical and chemical properties to those of the Cr element. The oxides of Ni and Cr are formed through the atomic diffusion process and combined with oxygen. Although Cr is more active than Ni, the diffusion rate of Ni is larger due to its smaller atomic radius; when Ni is oxidized, a p-type semiconductor of NiO film will be formed.

When the coating layer contains no Cr or a small amount of Cr, the formed NiO oxide film will be the main factor preventing the following oxidation process. With a higher content of Cr, however, the role of the Cr oxide film will be more pronounced, making the alloy coating enter the steady-state stage faster.

Figure 3 shows the oxidation weight gain curves of the alloy coatings with different Cr contents at 500°C. It can be seen that the measured curves show the similar increasing trend. The oxidation weight gain curves of the NiCrP alloy coating are relatively close, while that of the NiP alloy coating is obviously higher. Moreover, the curves of the Cr-containing alloy coatings exhibit a slower increase and then are gradually saturated, indicating the formation of the dense oxide films that can effectively prohibit the further oxidation process. However, the curve of NiP alloy coating shows a continuous increase, and does not reach the steady-state phase as observed in the oxidation weight gain curve measured at 400°C. This could be attributed to the higher oxidation temperature, at which it offers a larger thermal energy to accelerate the formation of a dense Cr oxide film on the coating surface, not only hindering the diffusion of oxygen in the air into the coating matrix, but also preventing the diffusion of the elements inside the coating to the surface. As a result, the following oxidation process has been remarkably delayed. As for the NiP alloy coating, the higher temperature of 500°C will induce a large internal stress in amorphous alloy coating, which inevitably results in stress cracking and pinhole defects in the formed oxide film and pinholes. In this case, the oxide film on the NiP coating surface will be no longer dense, thereby the internal oxidation process will occur, resulting in a significantly deteriorated oxidation resistance of the NiP amorphous alloy coating at 500°C.

The oxidation kinetics of NiP and NiCrP alloy coatings obey the exponent rate law at both 400 and 500°C, as shown in figures 2 and 3 and the measured oxidation curves can be fitted with the following equation [20,21]:

$$(\Delta G)^2 = K_p t \tag{1}$$

where ΔG is the weight gain per unit area of the specimens (mg cm^{-2}), K_p is the exponent rate constant (mg^2 cm^{-4} min^{-1}), and t is the oxidation time (min). The rate constant K_p can be derived by the following formula [22]:

$$K_p = A \exp^{-E_a/RT} \tag{2}$$

where A is a prefactor, E_a is the oxidative activation energy (J mol^{-1}), T is the absolute temperature (K), and R is the gas constant (8.314 J mol^{-1} K^{-1}). A and E_a values are calculated from the data shown in figures 2 and 3, and the derived oxidation rate equations for different alloy coatings are shown in table 1.

It can be seen from table 1, the NiP coating possesses the lowest E_a and the largest oxidation rate constant, revealing its poor high-temperature oxidation resistance. The related E_a can be substantially enlarged by adding Cr element, and thus the NiCr1.80P amorphous alloy coating exhibits the highest oxidation resistance in this study.

Table 1. Relationship between K_T and the oxidation temperature of the amorphous alloy coatings.

Coating	Oxidation rate equation
NiP	$K_T = 4.05 \times 10^{-2} \times \exp(-1.54 \times 10^3/RT)$
NiCr0.50P	$K_T = 2.43 \times 10^{-2} \times \exp(-8.16 \times 10^3/RT)$
NiCr0.80P	$K_T = 1.46 \times 10^{-1} \times \exp(-2.83 \times 10^4/RT)$
NiCr1.80P	$K_T = 2.31 \times 10^{-1} \times \exp(-3.53 \times 10^4/RT)$

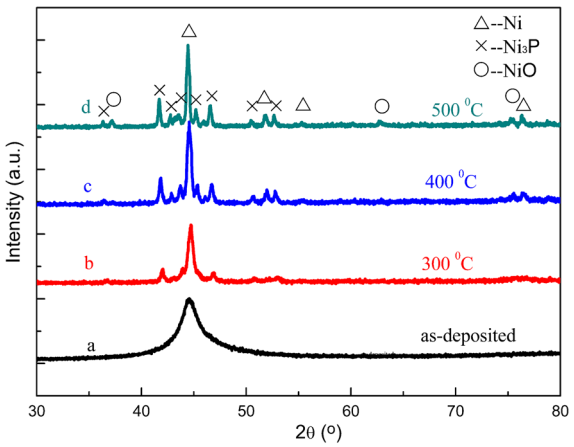

Figure 4. XRD patterns of (**a**) the as-deposited NiP coating, and isochronally heated to the completion temperature of (**b**) 300, (**c**) 400 and (**d**) 500°C, respectively.

Figure 4 shows the XRD patterns of the NiP amorphous alloy coating before and after being oxidized at different temperatures. As shown in figure 4a, the as-deposited NiP alloy coating has a broad diffraction peak at $2\theta \approx 45°$, indicating its amorphous structure. After being heated at 300°C for 10 h, the recorded main diffraction peak becomes sharper, as shown in figure 4b, which indicates that the amorphous–crystalline phase transition is undergoing in the alloy coating. However, the diffraction peak at $2\theta \approx 76°$ is still weak and broad, suggesting the crystallization process is far from completion, and the structure of the alloy plating layer should be between amorphous and crystalline.

After being heated at 400°C for 10 h, the observed diffraction peaks are quite sharp, as shown in figure 4c. Obviously, the alloy coating has become a crystalline structure. Compared to the sample treated at 300°C (figure 4b), both of the diffraction peaks corresponding to the Ni and Ni_3P phase are significantly enhanced. Moreover, a new peak appeared at $2\theta \approx 75.3°$ further demonstrates the precipitation of the NiO phase, which means a dense NiO film should be formed at the coating surface, leading to the best oxidization-resistance performance at 400°C, as shown in figure 2.

After being heated at 500°C for 10 h, as shown in figure 4d, the intensities of the diffraction peaks of Ni, Ni_3P and NiO are further sharpened, which indicate that the alloy coating has experienced a significant oxidation, and the alloy

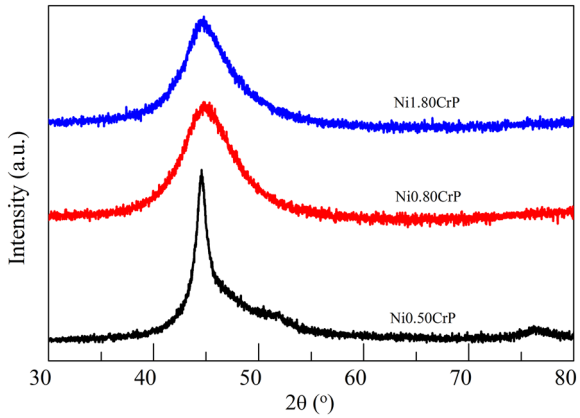

Figure 5. XRD patterns of NiCrP alloy coatings with different Cr contents.

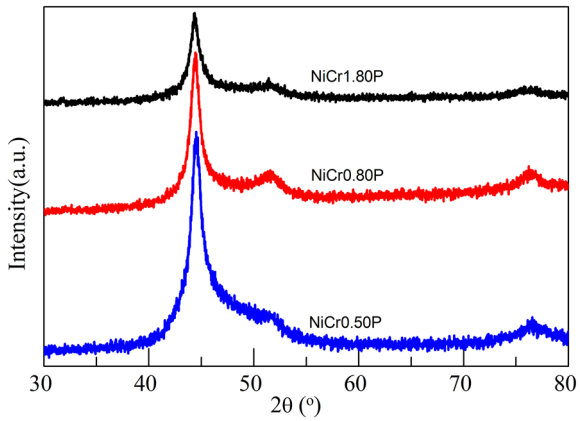

Figure 6. XRD patterns of NiCrP alloy coatings with different Cr contents after being oxidized at 300°C for 10 h.

coating has completely changed to a crystalline state. Guo and co-workers [23] also reported that when the holding temperature reaches 500°C, the NiP alloy coating will completely transform from amorphous to a crystalline structure. Meanwhile, the defects such as grain boundaries and segregation will appear in the coating, which makes the formed oxide film no longer dense, and thus the corresponding high-temperature oxidation resistance has been deteriorated to some extent, as shown in figure 3.

Figure 5 shows the XRD patterns of as-deposited NiCrP amorphous alloy coatings with different Cr contents. The measured diffraction peaks are located at $2\theta \approx 45°$, indicating that the as-deposited NiCrP alloy coatings are amorphous, which are similar to the NiP amorphous alloy coating as shown in figure 4a. Moreover, as the Cr content in the coating increases, the recorded diffraction peak becomes more and more diffuse, indicating that the gradual enhancement of the degree of structural disorder in the NiCrP alloy coatings due to the addition of Cr element.

Figure 6 shows the XRD patterns of the NiCrP amorphous alloy coatings after being oxidized at 300°C for 10 h. The diffraction peaks at $2\theta \approx 45°$ are slightly sharper than that

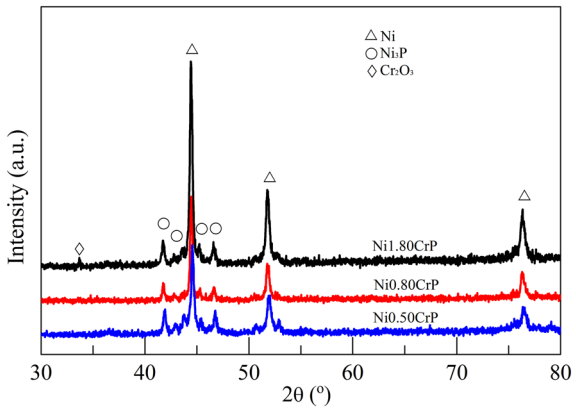

Figure 7. XRD patterns of NiCrP alloy coatings with different Cr contents after being oxidized at 400°C for 10 h.

of the as-deposited alloy coatings, but still of a diffuse feature, which indicates that the crystallization temperature of the NiCrP alloy coating is higher than 300°C. Compared with the NiP alloy coating oxidized under the identical condition (figure 4b), the addition of Cr element in the alloy coating can retain its amorphous structure under higher temperatures. Moreover, the diffraction peak of NiCr1.80P alloy coating is more diffuse than those of NiCr0.50P and NiCr0.80P, further confirming that the Cr content has a notable influence on the amorphous degree of the alloy coatings, which is consistent with the oxidation kinetics analyses presented above. Figure 7 shows the XRD patterns of the NiCrP alloy coatings after being oxidized at 400°C for 10 h. Unlike those shown in figures 5 and 6, the measured diffraction peaks are quite sharp, indicating the occurrence of the amorphous–crystalline phase transition in the alloy coatings. The characteristic diffraction peaks of the Ni_3P phase become detectable, but their intensities are still very low, which indicates that the alloy coatings have not been completely crystallized. Maeda *et al* [24] reported the similar results on an uncompleted crystallization of the amorphous alloy coating; after a heat preservation treatment at 400°C, there are still many free volumes anti-annealing and cannot be completely removed.

Moreover, a small peak at $2\theta = 33.5°$ has been detected in the XRD pattern of NiCr1.80P alloy coating, which can be assigned to the formed Cr_2O_3. When the content of Cr in the alloy coating is higher, it will be easier to form a relatively dense oxide film on the coating surface to protect the inside matrix of the alloy coating, thereby the NiCr1.80P alloy coating has an improved high-temperature resistance.

Figure 8 shows the XRD patterns of the NiCrP amorphous alloy coatings after being oxidized at 500°C. There are new phases in which NiO and CrO_3 precipitated, and the intensities of the diffraction peaks are obviously enhanced, indicating the degree of crystallization has been further improved. The as-deposited amorphous alloy coatings were almost completely oxidized and crystallized into Ni, Ni_3P, NiO and CrO_3 stable phases. When Cr content in the alloy coating increases,

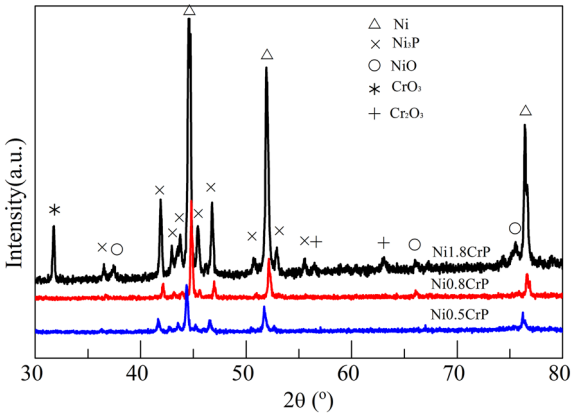

Figure 8. XRD patterns of NiCrP alloy coatings with different Cr contents after being oxidized at 500°C for 10 h.

more new phases are formed during the oxidation process, and the formed new phase is of a dense oxide film to protect the alloy coating from further oxidation. As a result, the higher the Cr content in the alloy coatings, the smaller the oxidation gain during the oxidation process, and the better the high-temperature oxidation resistance of the alloy coatings.

The atomic radius of Cr is larger than that of Ni, and the lattice constant of Ni increases when Cr is dissolved in the lattice of Ni, the 2θ in the XRD pattern shifts to a lower angle. Conversely, the atomic radius of O is smaller than that of Ni, resulting in a shift of the 2θ to a higher angle in the after forming NiO. In the oxidation process, Cr and O exist simultaneously in the alloy coating. Ni0.5CrP and Ni1.8CrP alloy coatings are relatively dense with less O, while Ni0.8CrP alloy coating is relatively loose with more O introduced. Therefore, the XRD spectra of Ni0.8CrP alloy shift to a high angle, and the XRD spectra of Ni0.5CrP and Ni1.8CrP alloy shift to a low angle.

4. Conclusion

According to the DSC curves of the alloy coatings, the onset temperature of crystallization is at 344.1°C for NiP amorphous alloy coating, began to crystallize, 375.4°C for NiCr0.50P coating, and 403.8°C for NiCr1.80P coating, respectively. The addition of Cr could effectively improve the crystallization temperature of the amorphous alloy coatings. With the increase of Cr content in the coating, the crystallization temperature significantly increased.

At high temperatures of 400 and 500°C, the increased oxidation weight of the NiP alloy coating is more than the NiCrP alloy coatings, indicating that the added Cr element can effectively improve the high-temperature oxidation resistance of the alloy coatings; as the Cr content increases, the oxidation resistance of the alloy coating can be further enhanced.

By analysing the XRD patterns of alloy coatings oxidized at different temperatures, NiP amorphous alloy coatings began to crystallize around 300°C, and the Ni_3P and Ni phases began to precipitate. However, the NiCrP alloy coating should retain amorphous at 300°C. The addition of Cr element increases the crystallization temperature of the NiCrP alloy coating. At higher temperatures, Cr combines with oxygen to form a compact Cr oxide film on the surface of the coating, which acts as a barrier to prevent the internal coating from being oxidized and improves its high-temperature oxidation resistance.

Acknowledgements

This work was supported by the National Key Laboratory Independent Research funding support project of China (Grant no. 20181-6).

References

[1] Brenner A and Riddel G 1964 *J. Res. Natl. Bur. Stand.* **37** 1
[2] Brenner A and Riddel G 1974 *J. Res. Natl. Bur. Stand.* **39** 385
[3] Li H, Chen H and Dong S 1998 *Appl. Surf. Sci.* **125** 115
[4] Novakovic J, Vassiliou P and Samara K 2006 *Surf. Coat. Technol.* **201** 895
[5] Song G-M, Wu Y and Xu Q 2010 *J. Power Sources* **195** 3913
[6] Wang A, Zhao C and He A 2016 *J. Alloys Compd.* **656** 729
[7] Xie J, Yang C and Duan M 2018 *Ceram. Int.* **44** 5459
[8] Honghong S and Jiaming J 2002 *Trans. Chin. Soc. Agric. Mach.* **1** 29
[9] Myshkin N K, Grigoriev A Y and Gutsev D M 2013 *Trans. Tech. Publ.* **527** 92
[10] Yang Q, Lv C and Huang Z 2018 *Int. J. Hydrog. Energy* **43** 7872
[11] Yu Y D, Wei G Y and Guo H F 2012 *Surf. Eng.* **28** 30
[12] Balaraju J N, Manikandanath N T and Grips V K W 2012 *Surf. Coat. Technol.* **206** 2682
[13] Hou P Y and Stringer J 1987 *J. Electrochem. Soc.* **134** 1836
[14] Hussey R J and Graham M J 1996 *Oxid. Met.* **45** 349
[15] Wang C Y, Zhou Y M and Zhang F L 2009 *J. Alloys Compd.* **476** 884
[16] Wu N, Li Y and Wang J 2012 *J. Mater. Process. Technol.* **212** 794
[17] Zhang B P, Habazaki H and Kawashima A 1991 *Corros. Sci.* **32** 433
[18] Kumar P S and Nair P K 1996 *J. Mater. Process. Technol.* **56** 511
[19] Wang Y and Lu K 2001 *Sci. China Ser. E (Tech. Sci.)* **44** 33
[20] Choi B Y, Liang J and Gao W 2005 *Met. Mater. Int.* **11** 499
[21] Erlinda V O, Daniel O B, Daniel E B, Silvina E F and Pablo R D 2017 *Environ. Sci. Pollut. Res.* **24** 27366
[22] Suwanwatana W, Yarlagadda S and Gillespie J J W 2003 *J. Mater. Sci.* **38** 565
[23] Lai Z H, Wu Y K and Guo K X 1984 *Acta Phys. Sin.* **33** 1182
[24] Maeda K, Ikari T and Akashi Y 1994 *J. Mater. Sci.* **29** 1449